Single-Layer Blue Organic Light-Emitting Diodes With Near-Unity Internal Quantum Efficiency

*Oskar Sachnik, Yungui Li, Xiao Tan, Jasper J. Michels, Paul W. M. Blom, and Gert-Jan A. H. Wetzelaer**

Efficient organic light-emitting diodes (OLEDs) commonly comprise a multilayer stack including charge-transport and charge- and exciton-blocking layers, to confine charge recombination to the emissive layer. Here, a highly simplified single-layer blue-emitting OLED is demonstrated based on thermally activated delayed fluorescence with the emitting layer simply sandwiched between ohmic contacts consisting of a polymeric conducting anode and a metal cathode. The single-layer OLED exhibits an external quantum efficiency of 27.7% with minor roll-off at high brightness. The internal quantum efficiency approaches unity, demonstrating that highly simplified single-layer OLEDs without confinement layers can achieve state-of-the-art performance, while greatly reducing the complexity of the design, fabrication, and device analysis.

1. Introduction

The first demonstration of electroluminescence in organic materials has driven the research of optoelectronic devices, such as organic light-emitting diodes (OLEDs), paving the way to mass-commercialization in display and lightning applications.[1] Early OLEDs employed a simple device structure by sandwiching the semiconducting layer between two electrodes, injecting holes into the organic semiconductor layer via the anode and electrons via the cathode. These countercharges are then transported through the organic semiconductor, where they meet and recombine via exciton formation and subsequent radiative decay, resulting in visible light emission. After the first demonstrations of electroluminescence in these simple OLEDs, considerable efficiency gains were made by increasing the number of functional layers and by harvesting triplet excitons.[2–6]

O. Sachnik, Y. Li, X. Tan, J. J. Michels, P. W. M. Blom, G.-J. A. H. Wetzelaer
Max Planck Institute for Polymer Research
Ackermannweg 10, 55128 Mainz, Germany
E-mail: wetzelaer@mpip-mainz.mpg.de

In these multilayer OLEDs, the light-emitting layer is surrounded by several charge-transport and charge- and exciton-blocking layers. By selecting materials with suitable charge-transport properties and appropriate energy levels for charges and excitons, these additional layers are used to transport charges to the emissive layer, in which charges and excitons are confined with the help of blocking layers.[2] As such, it is ensured that all charges and excitons recombine and decay within the emissive layer to maximize the internal quantum efficiency of the conversion of charges into photons. In addition, the emissive layer can be optimally positioned within the multilayer stack to reach maximum light outcoupling, thereby maximizing the external quantum efficiency (EQE). Typical maximum outcoupling efficiencies for multilayer OLEDs are in the 20% to 30% range, being the main limiting factor in the EQE of state-of-the-art multilayer OLEDs.[7,8]

However, a major drawback of multilayer OLEDs is their complexity in terms of design, fabrication, and interpretation. The additional transport and blocking layers have very specific requirements regarding energy levels, energy gap, and triplet energy, in order to minimize charge-injection barriers and enhance charge and exciton-blocking capabilities. This makes the design of a multilayer OLED cumbersome and induces additional fabrication steps, which drives up the costs. Furthermore, the additional heterojunctions frequently induce additional energy barriers and thus voltage losses, and these interfaces may be potential sources of device degradation. It is generally accepted that such complex device structures are required to achieve high EQEs in the 20%–30% range.[9,10] This then basically would rule out the realization of efficient OLEDs with a highly simplified structure consisting of a single emissive layer sandwiched between two electrodes, similar to the early OLEDs. Such a simplified structure is a prerequisite for solution-processed OLEDs due to stack integrity issues. A fundamental question therefore is what the maximum attainable efficiency in OLEDs with a simplified device structure would be and how it compares to the complex multilayer devices.

Recently, we demonstrated an efficient OLED with simplified device structure based on a yellow thermally activated delayed fluorescence (TADF) emitter.[11] In this OLED, the TADF emitter was sandwiched between two ohmic contacts, without any charge-transport or blocking layers. The ohmic

contacts, however, required the presence of tunneling interlayers, consisting of organic-semiconductor layers of a few nanometers thick. Although the requirements for these thin interlayers in terms of energy levels and triplet energies are far less elaborate than for conventional charge-transport layers, coating steps are still required to deposit these interlayers.[12] Not only is this suboptimal for vacuum-deposited OLEDs, but it would be an additional hurdle to overcome when aiming for fully solution-processed OLEDs.

For blue single-layer OLEDs, direct charge injection into the emitter via ohmic contacts becomes particularly challenging, since blue emitters have a large energy gap of approximately 3 eV. For emitters with a high ionization energy, efficient hole injection can be achieved with a combination of a high work function transition-metal oxide and a suitable tunneling interlayer, which, however, involves two vacuum-based deposition steps.[12] An alternative approach to achieve a high work function contact is to blend perfluorinated ionomers (PFI) with the conducting polymer poly(3,4-ethylenedioxythiophene) polystyrene sulfonate (PEDOT:PSS), which enhances the film work function up to 5.9 eV, as a result of the formation of a surface dipole, induced by a thin fluorine-rich overlayer.[13,14] Although higher efficiencies were reported for OLEDs containing PFI-modified hole-injection layers, as compared to standard PEDOT:PSS, it has been suggested that despite the high work function, these contacts are non-ohmic.[15,16] Direct evidence of the formation of an ohmic hole contact between PEDOT:PSS:PFI and high ionization energy (IE) organic semiconductors has indeed not been presented to date. Ohmic contacts are, however, of paramount importance for single-layer OLEDs to operate efficiently.

Herein, we first demonstrate that a blend film containing PEDOT:PSS and PFI in fact can provide ohmic hole injection into high-IE organic semiconductors. Subsequently, we present a single-layer blue-emitting TADF OLED, with the use of a spin-coated PFI-modified hole contact and a metal cathode. We demonstrate that the presence of a host in the emissive layer eliminates the need for an organic tunneling interlayer for ohmic electron injection. The device shows an external quantum efficiency of up to almost 28%, which equates to practically unity internal quantum efficiency when considering losses due to optical outcoupling, despite the absence of a charge- and exciton-confinement structure. We therefore show that highly simplified, single-layer OLEDs with zero electrical losses are a feasible alternative to state-of-the-art multilayer devices.

2. Results and Discussion

As a first step, we demonstrate ohmic hole injection from PEDOT:PSS:PFI into a high-IE organic semiconductor. The most direct way to demonstrate an ohmic hole contact, is the fabrication of a hole-only device with one of the contacts as an ohmic reference. In **Figure 1**, the current density-voltage characteristics of a hole only device of (9,10-bis(4-(9Hcarbazol-9-yl)−2,6-dimethylphenyl)−9,10-diboraanthracene (CzDBA) is displayed. CzDBA has a high IE of 5.93 eV.[17] The hole-only device consists of a PEDOT:PSS:PFI (1:6:14 by wt.) bottom contact and a C_{60}(4 nm)/MoO_3(10 nm)/Al top electrode. This top electrode has been shown to provide ohmic hole injection into a variety of organic semiconductors, including CzDBA, and is therefore
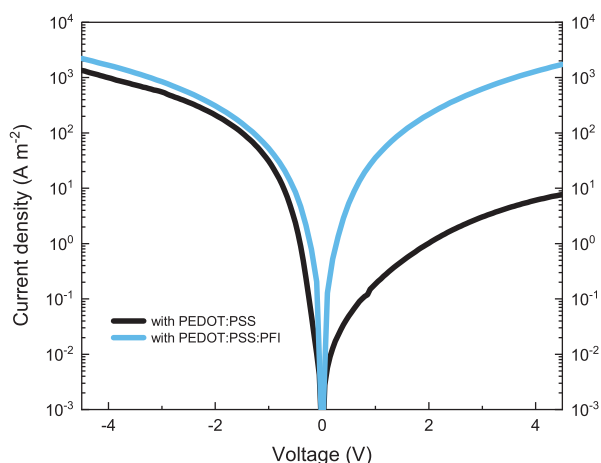

Figure 1. Ohmic hole injection from a PFI-modifed anode. Current density (J) versus voltage (V) characteristics of a hole-only device of CzDBA (80 nm) with a HIL/CzDBA/C_{60}/MoO_3/Al device structure where the hole-injection layer (HIL) is either PEDOT:PSS or PEDOT:PSS:PFI. At negative bias, current is injected from the ohmic C_{60}/MoO_3 top contact. Positive bias corresponds to hole injection from the bottom HIL. The symmetric $J-V$ characteristic is indicative of ohmic hole injection from PEDOT:PSS:PFI, while the injected hole current from PEDOT:PSS is substantially reduced due to the injection barrier.

an ideal reference.[11,12] As shown in Figure 1, symmetric $J-V$ characteristics are observed, indicating that hole injection from PEDOT:PSS:PFI under forward bias is equally efficient to injection from the ohmic top electrode under reverse bias. A control device with a standard PEDOT:PSS bottom contact shows an injected current that is >2 orders of magnitude lower as a result of the hole-injection barrier due to the work-function mismatch. The current under reverse bias is practically unaltered, indicating that the PEDOT:PSS:PFI layer does not give rise to additional electrical resistance. Therefore, it can be concluded that hole injection from PEDOT:PSS:PFI into CzDBA is ohmic. To further validate that a truly ohmic hole contact is formed with the simple PEDOT:PSS:PFI layer, we fabricated a single-layer OLED of CzDBA which reached an EQE of ≈18% (Figure S1b, Supporting Information), which is close to the reported value of 19% for an ohmic MoO_3/C_{60} bottom contact, while exhibiting similarly low operating voltages.[11]

The demonstration of ohmic hole injection from PEDOT:PSS:PFI into a high-IE organic semiconductor shows promise for blue-emitting single-layer OLEDs. The fabrication of efficient blue-emitting OLEDs in general is challenging, because the wide energy gap of blue emitters complicates efficient charge injection. Furthermore, charge and exciton confinement in multilayer blue OLEDs requires wide-gap transport and blocking layers with high triplet energies, which makes material selection more cumbersome. In a single-layer OLED, these blocking and transport layers are absent, thereby greatly simplifying the device design.

To investigate the possibility of fabricating highly efficient blue-emitting OLEDs in a single-layer architecture, we chose SpiroAc-TRZ (10-(4-(4,6-diphenyl-1,3,5-triazin-2-yl)phenyl)-10H-spiro[acridine-9,9′-fluorene] as a blue-emitting organic semiconductor, which exhibits TADF.[18] SpiroAc-TRZ has been

ADVANCED
SCIENCE NEWS
www.advancedsciencenews.com
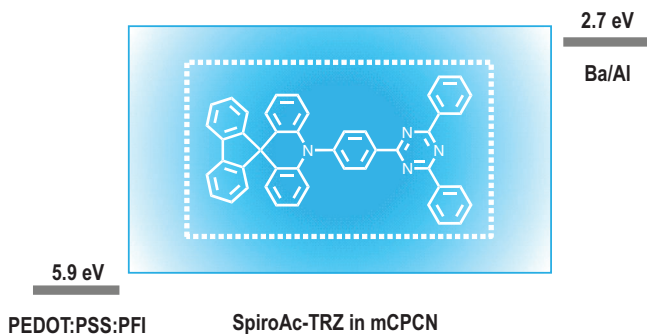
ADVANCED
MATERIALS
www.advmat.de

Figure 2. Device layout of a SpiroAc-TRZ single-layer OLED. The emissive layer comprising evaporated SpiroAc-TRZ:mCPCN (1:1) is sandwiched between a PEDOT:PSS:PFI bottom anode and a barium/aluminum top cathode. The work functions of the electrodes and the chemical structure and energy levels of SpiroAc-TRZ are indicated.

successfully applied in multilayer OLEDs and has favorable properties, such as a high photoluminescence quantum yield of up to 100% and a highly horizontal dipole orientation when doped in a mCPCN (9-(3-(9H-carbazol-9-yl)phenyl)-9H-carbazole-3-carbonitrile) host matrix.[18,19] The mCPCN host has a larger band gap and higher triplet energy than the SpiroAc-TRZ emitter, and in the chosen host-to-guest ratio of 1:1, charge transport is expected to be solely taking place on the emitter, i.e., guest-to-guest transport. A photoluminescence quantum yield (PLQY) of 97% was measured for a 1:1 host-guest ratio. **Figure 2** shows the device layout of our single-layer OLED, using a spin-coated layer of PEDOT:PSS:PFI as a hole contact, a co-evaporated active layer of SpiroAc-TRZ and mCPCN, and an electron contact comprising a thin layer of barium (2.5 nm) capped with aluminum (100 nm).

In such a simple device architecture, balanced electron and hole transport is a prerequisite to achieve an optimal recombination zone close to the center of the emissive layer. To characterize the electron and hole transport, we fabricated electron- and hole- only devices of the co-evaporated layer. Hole-only devices were fabricated using a PEDOT:PSS:PFI/SpiroAc-TRZ:mCPCN(1:1)/C_{60}/MoO$_3$/Al device layout, with the C_{60}(3 nm)/MoO$_3$/Al top electrode as a proven ohmic hole contact.[12] The J–V characteristics are symmetric in voltage, indicating that injection from PEDOT:PSS:PFI is as efficient as injection from the ohmic top contact (Figure S2, Supporting Information). Electron-only devices were fabricated using two low-work-function contacts in a Al/SpiroAc-TRZ:mCPCN(1:1)/Ba (5 nm)/Al layout. Intriguingly, while in previous single-layer OLEDs an ohmic electron contact required a thin (4 nm) 2,2″,2‴-(1,3,5-benzinetriyl)-tris(1-phenyl-1-H-benzimidazole) (TPBi) interlayer, it could here be omitted without compromising electron injection (Figure S3a, Supporting Information).[11] We hypothesize that the presence of a wide-gap host pre-empts the need for an interlayer with a high LUMO, as the presence of the (high-LUMO) host molecules near the top interface could facilitate electron injection into the emitter similar to the case of a thin interlayer tunneling barrier. This hypothesis is confirmed by fabricating electron-only devices based on neat SpiroAc-TRZ with and without a TPBi interlayer. In the absence of a host, a large injection barrier is present when omitting

the TPBi interlayer, despite the low work function of barium of 2.7 eV, which should be sufficient to align the electrode Fermi level with the LUMO of SpiroAc-TRZ (Figure S3b, Supporting Information).[20] This confirms that the host assists in electron injection into the emitter, which would allow for further simplification of the single-layer OLED, by omitting the tunneling interlayer for electron injection.

The comparison of the electron and hole current (**Figure 3**a) shows balanced charge transport. To quantify the charge-transport parameters, both currents were fitted with a drift-diffusion model, in which the mobility is incorporated according to the extended Gaussian disorder model (Table S1, Supporting Information).[21,22] The mobility for both holes and electrons amounts to 5.6×10^{-9} cm^2 V^{-1} s^{-1} in the limit of vanishing electric field and charge concentration. The hole current can be simulated without additional charge traps. The electron current shows minor electron trapping with a trap density of 2.0×10^{16} cm^{-3}. This can be observed from the stronger voltage dependence of the current at low voltage, prior to reaching the trap-filled limit at ≈1 V.[23] Charge transport via the emitter is balanced and is dominated by guest-to-guest hopping in the 1:1 host to guest ratio (Figure S4, Supporting Information). Based on the charge-transport characteristics, the recombination profile of a single-layer OLED can be simulated (Figure 3b). Owing to the balanced charge transport, the recombination profile has its maximum close to the center of the active layer, which is expected to be beneficial for the efficiency, and remains fairly constant beyond an operating voltage of 2.5 V.

Considering the balanced charge transport and the fact that ohmic hole and electron injection can be achieved with a simple polymeric anode and a metallic cathode, all prerequisites for a highly simplified blue single-layer OLED appear to be in place. Therefore, a single-layer OLED based on SpiroAc-TRZ was fabricated using the device structure as displayed in Figure 2. The current density-luminance-voltage characteristics are shown in **Figure 4**a, and the corresponding EQE and power efficiency are displayed in Figure 4b as a function of brightness. The OLED exhibits sky-blue light emission with an electroluminescence spectrum peaking at 490 nm (inset Figure 4b) and reaches an impressive maximum EQE of 27.7%. A luminance of 100 cd m^{-2} is already reached at 3.1 V, only slightly exceeding the magnitude of the optical energy gap of 2.88 eV. As a result of the high EQE and the low operating voltage, the device reaches a maximum power efficiency of 85 lm W^{-1}. In addition, the efficiency roll-off is relatively small, maintaining a high EQE of 23% even at a luminance of 1000 cd m^{-2}. The turn-on voltage at 1 cd m^{-2} equals 2.53 V, which is lower than the optical gap of 2.88 eV (Figure S5, Supporting Information), which can be traced back to the recombination of diffused and thermally generated charge carriers below the built-in voltage, the concentration of which is maximized due to the ohmic contacts.[24] For this reason, single-layer OLEDs with ohmic contacts are capable of operating at very low voltages. A control device with a non-ohmic PEDOT:PSS electrode reaches an EQE of 14% (Figure S6, Supporting Information), after electrical conditioning. The device-performance parameters are summarized in Table S2 (Supporting Information). These device characteristics are on par with state-of-the-art multilayer OLEDs, with the difference that here the performance is achieved with an emissive layer simply sandwiched between a
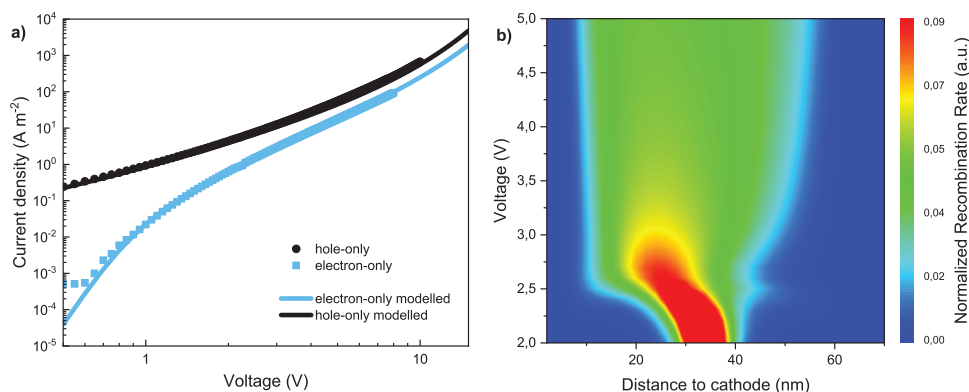
Figure 3. Charge-transport characteristics and simulated recombination profile. a) Current density–voltage characteristics of SpiroAc-TRZ:mCPCN (1:1) electron- and hole-only devices (symbols) and simulated currents (lines), with a layer thickness of 105 nm. b) Recombination profile normalized to the integrated rate for a SpiroAc-TRZ:mCPCN double-carrier device with a layer thickness of 70 nm.

polymeric anode and a metal cathode, without any (high triplet energy) charge- or exciton blocking layers. The highly reduced complexity of the device both in terms of the amount of materials and the number of layers is very attractive for the fabrication, design and analysis of OLEDs.

Despite the obvious benefits of such a simple device layout, a question that may arise is whether the absence of blocking layers would compromise the device performance, as such additional layers have been crucial in the development of OLEDs over recent years. To assess such potential performance losses, we analyzed the internal quantum efficiency by means of optical outcoupling simulations.[8,25] The model simulates the fraction of light that is emitted to air and incorporates the measured optical constants of all layers including the co-evaporated SpiroAc-TRZ:mCPCN (1:1) film (Figure S7, Supporting Information), as well as the horizontal dipole orientation of the emitter of 83% (Figure S8a, Supporting Information), as was also obtained previously for this system.[18] The maximum simulated optical outcoupling efficiency for a device with an optimized 80 nm SpiroAc-TRZ:mCPCN layer equals ≈27% (Figure S9, Supporting Information), similar to what has previously been obtained for light outcoupling in single-layer OLEDs.[25] The fact that the outcoupling efficiency matches the measured EQE implies that the internal quantum efficiency

approaches unity. Therefore, even without blocking layers, no charges or excitons are lost by surface recombination or quenching at the electrodes.

The addition of a 20 nm hole- and exciton-blocking layer between the emissive layer and the cathode did not improve the EQE (Figure S10, Supporting Information), confirming that nonradiative losses near the metallic cathode are absent. Indeed, it has been demonstrated that such nonradiative losses are fully suppressed for truly ohmic contacts,[26] as have been used in our blue single-layer OLED. Near ohmic contacts, the charge density of majority carriers is high (Figure S11, Supporting Information), such that minority carriers cannot escape the device without recombining. This can also be seen from the simulated recombination profile in Figure 3b, where the recombination rate goes to zero near the electrode interfaces, implying no leaking of minority carriers into the electrodes. In Figure S11 (Supporting Information), it is demonstrated that the simulated electrical efficiency, defined as number of formed excitons per injected charge, equals unity, rationalizing the high internal quantum efficiency. Additionally, the EQE is temperature independent (Figure S12, Supporting Information), which further excludes potential nonradiative losses, such as exciton-polaron quenching. The realization of a single-layer OLED with zero electric loss demonstrates that there is no fundamental efficiency deficit with regard to
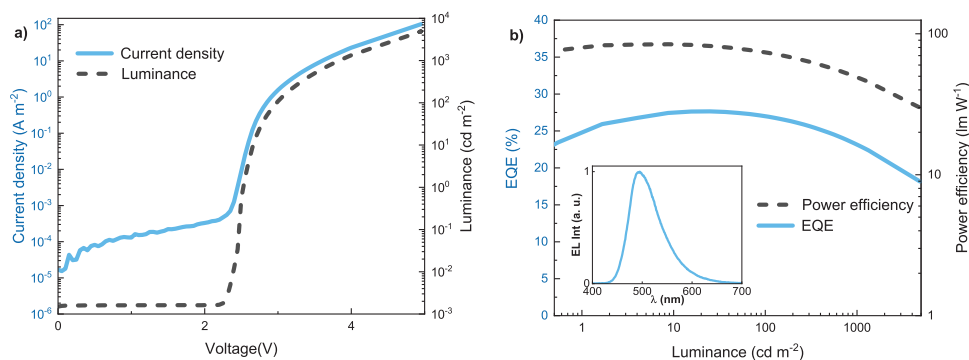

Figure 4. Device performance of a single-layer SpiroAc-TRZ:mCPCN (1:1) OLED. a) Current density–voltage and luminance–voltage characteristics of a single-layer SpiroAc-TRZ:mCPCN (1:1) OLED with an emissive-layer thickness of 77 nm. b) EQE and power efficiency versus luminance. Inset: electroluminescence spectrum with a maximum at 490 nm.

2300574 (4 of 6)

**ADVANCED
SCIENCE NEWS**

www.advancedsciencenews.com

**ADVANCED
MATERIALS**

www.advmat.de

complex multi-layer structures and paves the way for future highly efficient printed OLEDs.

3. Conclusion

We have demonstrated that a highly efficient and simple sky-blue OLED can be accomplished with one layer of light-emitting material between two ohmic contacts. The OLED consists of a layer of a TADF emitter blended with a host in equal ratios, sandwiched between a PEDOT:PSS:PFI hole contact and a metal top electrode, without any additional interlayers. It was verified that these contacts provide ohmic charge injection, leading to a highly simplified single-layer OLED with 27.7% EQE and low operating voltage, with a low efficiency roll-off at high brightness. Using optical outcoupling simulations, it was demonstrated that the device exhibits close to 100% internal quantum efficiency, establishing that additional charge- and exciton-blocking layers are not needed in a single-layer OLED with ohmic contacts. Therefore, our work demonstrates that a very simple device architecture with a greatly reduced number of materials and coating steps can rival current multilayer OLEDs. The solution-processed hole contact even lays the foundations for efficient fully solution-processed single-layer OLEDs. Not only is this highly simplified single-layer OLED structure advantageous from the perspective of device design and fabrication, but it is also of great benefit for developing understanding of the device physics, which is complicated in multi-layer architectures due to the multitude of materials and hetero-junctions and associated energy barriers, of which the charge-transport and barrier-height parameters are rarely known sufficiently precise for a meaningful analysis.

4. Experimental Section

Materials: SpiroAc-TRZ was synthesized according to literature and purified by sublimation.[18] Nafion (PFI) was purchased from Sigma Aldrich as 5 wt.% solution in a mixture of lower aliphatic alcohols and water, containing 45% water. mCPCN, TPBi and C_{60} were purchased in sublimed grade from Ossila BV.

Device Fabrication: OLED devices were fabricated on glass substrates prepatterned with ITO. The substrates were cleaned by washing with detergent solution and ultrasonication in acetone (5 min) and isopropyl alcohol (5 min), followed by UV–ozone treatment (50 min). PFI-containing blends were prepared 24 h prior to device fabrication by mixing PEDOT:PSS (CLE-VIOS P VP AI 4083) with Nafion® in a 1:6:14 ratio and diluted in deionized water (1:1). PEDOT:PSS:PFI was applied by spin coating, resulting in films of 20 nm thickness, which were subsequently annealed at 130 °C for 12 min. The substrates were then transferred to a nitrogen-filled glove box. Thermal evaporation of the emissive layer was performed at a base pressure of 2×10^{-6} to 3×10^{-6} mbar. Barium (2.5 nm) and aluminum (100 nm) were evaporated to finalize the top contact. For hole-only devices, a top contact consisting of C_{60} (4 nm), MoO_3 (10 nm) and aluminum (100 nm) was evaporated.

For electron-only devices, aluminum (30 nm) was thermally evaporated on cleaned glass substrates, followed by thermal evaporation of a layer of the organic semiconductor and an optional TPBi (4 nm) interlayer. Barium (5 nm) and aluminum (100 nm) were evaporated to finalize the device.

Measurements: Electrical characterization was carried out under nitrogen atmosphere with a Keithley 2400 source meter and light output was recorded with a Si photodiode with NIST-traceable calibration, with a detector area (1 cm²) larger than the emitting area of the OLED[27] (0.16 cm²). The photodiode was placed close to (but not in contact with) the OLED to capture all photons emitted in a forward hemisphere. To avoid any light detection emitted from the substrate edges, the edges were masked by the sample holder and the substrate size (3 × 3 cm²) was considerably larger than the photodetector area. The EQE, the luminance and power efficiency were calculated from the measured photocurrent, the device current, and the electroluminescence spectrum. Electroluminescence spectra were obtained with a USB4000-UV–vis-es spectrometer.

Supporting Information

Supporting Information is available from the Wiley Online Library or from the author.

Conflict of Interest

The authors declare no conflict of interest.

Data Availability Statement

The data that support the findings of this study are available from the corresponding author upon reasonable request.

[1] C. W. Tang, S. A. Vanslyke, *Appl. Phys. Lett.* **1987**, *51*, 913.

[2] J. Kido, M. Kimura, K. Nagai, *Science (80-.).* **1995**, *267*, 1332.

[3] H. Uoyama, K. Goushi, K. Shizu, H. Nomura, C. Adachi, *Nature* **2012**, *492*, 234.

[4] C. Adachi, M. A. Baldo, M. E. Thompson, S. R. Forrest, *J. Appl. Phys.* **2001**, *90*, 5048.

[5] Y. Liu, C. Li, Z. Ren, S. Yan, M. R. Bryce, *Nat. Rev. Mater.* **2018**, *3*, 18020.

[6] K. Walzer, B. Männig, M. Pfeiffer, K. Leo, *Chem. Rev.* **2007**, *107*, 1233.

[7] S. Y. Kim, J. J. Kim, *Org. Electron.* **2010**, *11*, 1010.

[8] M. Furno, R. Meerheim, S. Hofmann, B. Lüssem, K. Leo, *Phys. Rev. B: Condens. Matter Mater. Phys.* **2012**, *85*, 115205.

[9] J. W. Sun, J. H. Lee, C. K. Moon, K. H. Kim, H. Shin, J. J. Kim, *Adv. Mater.* **2014**, *26*, 5684.

[10] Q. Zhang, D. Tsang, H. Kuwabara, Y. Hatae, B. Li, T. Takahashi, S. Y. Lee, T. Yasuda, C. Adachi, *Adv. Mater.* **2015**, *27*, 2096.

[11] N. B. Kotadiya, P. W. M. Blom, G. J. A. H. Wetzelaer, *Nat. Photonics* **2019**, *13*, 765.

[12] N. B. Kotadiya, H. Lu, A. Mondal, Y. Ie, D. Andrienko, P. W. M. Blom, G. J. A. H. Wetzelaer, *Nat. Mater.* **2018**, *17*, 329.

[13] T. W. Lee, Y. Chung, O. Kwon, J. J. Park, *Adv. Funct. Mater.* **2007**, *17*, 390.

[14] Z. Zhong, Y. Ma, H. Liu, F. Peng, L. Ying, S. Wang, X. Li, J. Peng, Y. Cao, *ACS Appl. Mater. Interfaces* **2020**, *12*, 20750.

[15] Y. H. Kim, C. Wolf, H. Cho, S. H. Jeong, T. W. Lee, *Adv. Mater.* **2016**, *28*, 734.

[16] D. Belaineh, J. K. Tan, R. Q. Png, P. F. Dee, Y. M. Lee, B. N. N. Thi, N. S. Ridzuan, P. K. H. Ho, *Adv. Funct. Mater.* **2015**, *25*, 5504.

[17] T. L. Wu, M. J. Huang, C. C. Lin, P. Y. Huang, T. Y. Chou, R. W. Chen-Cheng, H. W. Lin, R. S. Liu, C. H. Cheng, *Nat. Photonics* **2018**, *12*, 235.

[18] T. A. Lin, T. Chatterjee, W. L. Tsai, W. K. Lee, M. J. Wu, M. Jiao, K. C. Pan, C. L. Yi, C. L. Chung, K. T. Wong, C. C. Wu, *Adv. Mater.* **2016**, *28*, 6976.

[19] M. S. Lin, S. J. Yang, H. W. Chang, Y. H. Huang, Y. T. Tsai, C. C. Wu, S. H. Chou, E. Mondal, K. T. Wong, *J. Mater. Chem.* **2012**, *22*, 16114.

[20] K. C. Mishra, R. Garner, P. C. Schmidt, *J. Appl. Phys.* **2004**, *95*, 3069.

[21] W. F. Pasveer, J. Cottaar, C. Tanase, R. Coehoorn, P. A. Bobbert, P. W. M. Blom, M. De Leeuw, M. A. J. Michels, *Phys. Rev. Lett.* **2005**, *94*, 206601.

[22] L. J. A. Koster, E. C. P. Smits, V. D. Mihailetchi, P. W. M. Blom, *Phys. Rev. B: Condens. Matter Mater. Phys.* **2005**, *72*, 085205.

[23] W. Kao, K.-C. Hwang, *Electrical Transport in Solids*, Pergamon Press, Oxford, UK **1981**.

[24] Y. Li, O. Sachnik, B. van der Zee, K. Thakur, C. Ramanan, G. J. A. H. Wetzelaer, P. W. M. Blom, *Adv. Opt. Mater.* **2021**, *9*, 2101149.

[25] Y. Li, N. B. Kotadiya, B. van der Zee, P. W. M. Blom, G. J. A. H. Wetzelaer, *Adv. Opt. Mater.* **2021**, *9*, 2001812.

[26] G. J. A. H. Wetzelaer, P. W. M. Blom, *ACS Appl. Mater. Interfaces* **2022**, *14*, 7523.

[27] S. R. Forrest, D. D. C. Bradley, M. E. Thompson, *Adv. Mater.* **2003**, *15*, 1043.

2300574 (6 of 6)